SCLEROTIC RIB METASTASES DETECTION ON ROUTINE CT IMAGES

Jianhua Yao[1], Joseph E. Burns[2], and Ronald M. Summers[1]

[1]Imaging Biomarkers and Computer-Aided Diagnosis Laboratory, Radiology and Imaging Sciences, Clinical Center, National Institutes of Health

[2]Department of Radiological Sciences, University of California, Irvine, School of Medicine

ABSTRACT

This work presents a computer-aided detection (CAD) system to aid radiologists in finding sclerotic bone metastases in the ribs on routine body imaging CT protocols with 5mm chest/abdomen CT images. First, the spine is segmented to locate the ribs using thresholding, region growing and a vertebra template. The centerlines of ribs are then traced by a progressive algorithm based on maximizing the cross-section overlap. The profile of the ribs along the centerline is analyzed to generate the initial detections. A set of quantitative features is then extracted and sent to a support vector machine for classification. Novel visualization techniques are also developed to display all ribs and the distribution of bone lesions in one single view. The system was tested on 10 data sets with 185 sclerotic lesions identified by an expert. A leave-one-out cross-validation results in 75.4% sensitivity at an average of 5.6 false positives per case.

Index Terms— computer aided detection, bone metastasis, sclerotic lesion, ribs

1. INTRODUCTION

Significantly associated with cancer, bone metastasis with occur in up to 70% of people afflicted with advanced prostate and breast cancer alone. Approximately 350,000 people in the United States die each year with bone metastases [1]. Bone metastases can result in severe bone pain and pathological fractures, as well as associated spinal cord and other nerve compression [1]. Moreover, after the initial discovery of the metastasis, no more than 20% of breast cancer patients survive more than five years [1]. Early detection of bone metastases thus has substantial clinical prognostic importance. Significantly, over 90% of bone metastases are in the spine, ribs, pelvis and skull [1]. We have developed a system to detect bone metastasis in spine [2]. This investigation focuses on the detection of sclerotic bone lesions in the ribs.

Sclerotic metastases consist of ectopocally placed relatively focal regions of abnormally hyperdense bone [1]. They are believed to develop density through the production of growth factors that encourage osteoblast proliferation, differentiation, and bone formation. Rib lesions are often missed during CT Interpretation. Oversight of lesions may be due to any one of several reasons, or a combination. First, there could be many lesions distributed among 12 pairs of ribs; second, ribs cross the transverse image plane at oblique angles which make the detection difficult; and third, rib cross sections are usually small relative to the field of view, as well as multifocal and eccentrically distributed on each image (or many to be interpreted) complicating the problem of visual perception and lesion detection. Furthermore, identifying the location of the lesion (i.e. on which rib) is not a trivial task since it involves tracing back to the spine and counting. Therefore, it is desirable to have a computer system which can assist radiologists detecting the rib lesions and identifying their location. Figure 1 shows a few examples of sclerotic rib metastases.

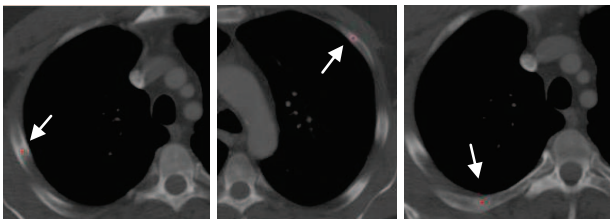


Figure 1. Examples of sclerotic rib lesions.

Several investigations have been conducted to segment ribs on CT images. Staal et al. [3] proposed a framework for automatic rib segmentation and labeling. They extracted 1D ridges from the image, grouped them into a centerline and applied region growing using the centerlines as initial points from which to segment the ribs. Klinder et al. [4] adapted a pre-computed rib cage model to the CT data based on a ray-searching technique. Lee et al. [5] segmented individual ribs from low-dose CTs using a cylindrical template for rib growing. Kiraly et al. [6] developed a new visualization technique by straightening the rib along the centerline. Shen et al. [7] proposed a cross-sectional plane scheme to detect rib metastasis. All the above mentioned techniques for rib segmentation and lesion detection require thin-cut continuous slices, where the CT images are reconstructed at 1 to 2 mm thickness and spacing. However, thin-section CT often requires greater radiation dose and is usually not obtained for most patients. Instead, routine chest/abdomen CT examination protocols commonly used in clinical

practice utilize 5 mm slice thickness and spacing. These thicker CT sections pose great challenges to image processing of ribs due to the partial-volume effect. Some ribs may appear disconnected, and other bones such as the scapula may be fused with the ribs. The objective of our investigation is to develop a computer-aided detection system for sclerotic rib lesions on routine chest and abdomen CT studies, and develop tools for intuitive rib and lesion visualization.

2. METHOD OVERVIEW

The outline of our approach is illustrated in Figure 2. First, the spine is segmented; second, the rib centerline is traced and detected; third, ribs are segmented and visualized; fourth, lesion candidates are detected based on signal processing on the profile of ribs along the centerline; and fifth, quantitative features are computed and sent to a support vector machine for classification.

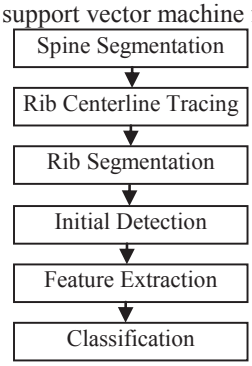


Figure 2. Flow chart

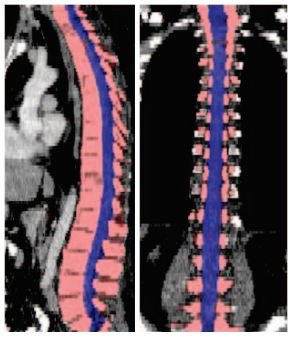


Figure 3. Spine segmentation

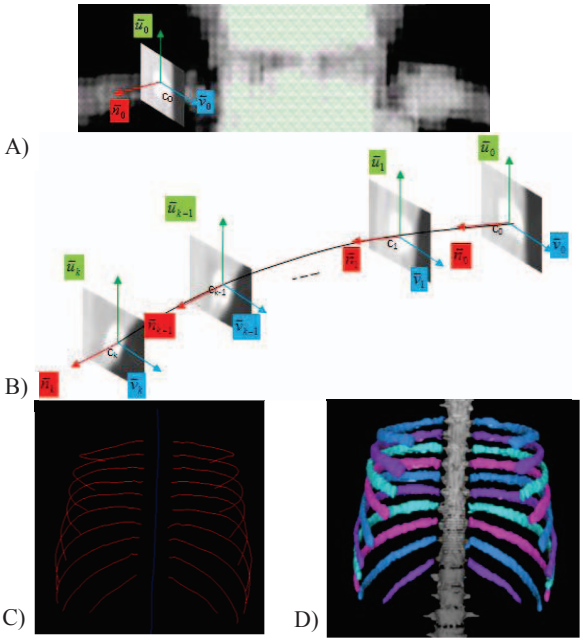


Figure 4. Rib tracing and segmentation. A) Initialization; B) Progressive tracing; C) Rib centerlines; D) Segmentation and labeling results.

3. SPINE SEGMENTATION

We used a spine segmentation algorithm developed in a previous study [8]. After segmenting and localizing the spine via thresholding and region growing, we extract the spinal canal using a directed graph. The vertebra borders are further refined using a vertebra template. Figure 3 shows the spine segmentation results.

4. RIB TRACING AND VISUALIZATION

The ribs stem from the thoracic spine. We propose a scheme that traces the ribs one-by-one from the segmented spine. The scheme has three stages: first, the initialization locates the starting tracing point for each rib candidate; second, a progressive tracing algorithm iteratively advances the rib along the centerline until the entire rib is traced; and third, false rib candidates are eliminated.

In the initialization stage, bony structures (HU value greater than 200) in the immediate neighborhood (within 2 cm) of the segmented spine are first detected. At the centroid of each detection, a cross section is defined as f_0,

$$f_0 = (c_0 \;\; \bar{n}_0 \;\; \bar{u}_0 \;\; \bar{v}_0) \tag{1}$$

where c_0 is the center of the cross section, $\bar{n}_0$ is the normal, $\bar{u}_0$ and $\bar{v}_0$ form the in-plane coordinate system. f_0 is determined by minimizing the bony area in the cross section.

$$f_0 = \arg\min A(f) \tag{2}$$

where A is the bony area in the cross section. The initialization process is illustrated in Figure 4a.

Since classic region growing technique is not sufficient to trace the ribs on 5 mm routine CT images, a progressive cross section advancing algorithm is proposed. Assuming the first *k-1* cross sections f_0, f_1, …, f_{k-1} are already calculated, the following procedures are carried out to obtain the k^{th} cross section, $f_k = (c_k \;\; \bar{n}_k \;\; \bar{u}_k \;\; \bar{v}_k)$.

1. a B-spline curve is fit for the current centerline (c_0, c_1, …, c_{k-1}).
2. $\bar{n}_k$ is set as the tangent at c_{k-1} of the B-spline curve.
3. $\bar{u}_{k-1}$ and $\bar{v}_{k-1}$ are projected onto the $\bar{n}_k$ plane to get $\bar{u}_k$ and $\bar{v}_k$, i.e.,
$$\bar{u}_k = \bar{u}_{k-1} - \bar{n}_k \cdot (\bar{u}_{k-1} \circ \bar{n}_k)$$
$$\bar{v}_k = \bar{v}_{k-1} - \bar{n}_k \cdot (\bar{v}_{k-1} \circ \bar{n}_k) \tag{3}$$
4. The center of cross section f_k is predicted as
$$c_k' = c_{k-1} + \bar{n}_k \cdot s \tag{4}$$
where s is the tracing step size, which is set as the in-plane pixel size of the CT slice.
5. The pixel values on the cross section f_k are obtained by tri-linear interpolation from the original 3D CT image. The pixel size is $s*s$. After that, the centerline location c_k is determined by maximizing the overlap of bone

pixels (HU values greater than 200) between f_k and f_{k-1} and minimizing the distance between c_k and c_k', i.e.

$$c_k = \arg\max\left(O(f_k, f_{k-1}) - \|c_k' - c_k\|\right) \quad (5)$$

The above procedure is repeated until no more bone pixels are found on the cross section. The progressive tracing procedure is illustrated in Figure 4b. After this, (c_0, c_1, .., c_n) form the centerline of the rib.

In the last stage, false rib centerlines are eliminated based on two criteria. First, centerline shorter than a threshold (the width of the vertebra in current method) will be eliminated; and second, if there are more than two detected rib centerlines on one side of a particular vertebra, the shorter one will be eliminated. The traced rib centerlines and the cross sections are shown in Figure 4C and 4B.

The rib segmentation is achieved by stacking all the cross sections and back-projecting to the original CT data. For any rib pixel (x_i, y_i) on cross section f_k, the corresponding pixel $p_{i,k}$ in 3D CT coordinate is

$$p_{i,k} = c_k + x_i \cdot \vec{u}_k + y_i \cdot \vec{v}_k \quad (6)$$

The segmented pairs of ribs (left and right) are then ordered and labeled by their attaching vertebrae from T1 to T12. Figure 4d shows the segmented ribs with alternating colors.

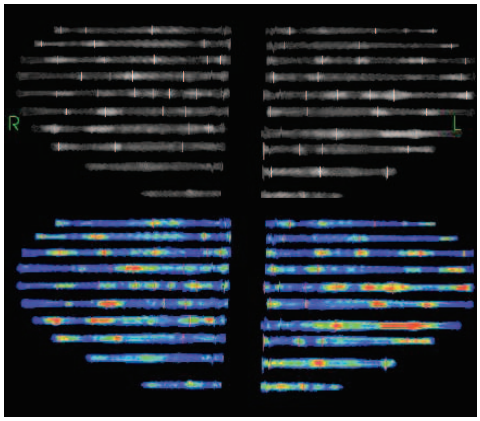


Figure 5. Whole rib maps. Vertical bars indicates manually labeled lesions. A) Intensity integral map; B) Hot-cool color map.

We develop a novel way to visualize all ribs in one view following the idea proposed in [6]. A rib is first straightened using its centerline, then the straightened rib is projected to a rectangular region. The projected ribs are arranged in vertical order from T1 to T12. Left and right ribs are separated. Different projection schemes, such as maximum intensity projection (MIP) or intensity integral can be applied to generate different rib maps. Figure 5 shows the whole rib maps. We use a hot-cool color map to enhance the visual effect. Since sclerotic lesions have high density, they appear to be highlighted segments in the rib map. We also superimpose the visually identified lesions by a radiologist on the rib map to demonstrate the distribution of rib lesions. It can be noted that the lesions mostly coincide with the high intensity (hot) regions on the rib map, which can be readily appreciated in one glance.

5. RIB LESION DETECTION

To detect potential rib lesions, we compute the profiles along the centerline using the cross section images. The value on the profile can be pixel intensity, rib diameter or cortical bone thickness. Figure 6A shows an example of an intensity profile. Visually identified lesions are indicated on the profile, which correspond to local peaks on the profile. We analyze the profiles for local peaks using signal processing techniques.

The rib profile is first smoothed using a Gaussian filter to reduce noise. The local peaks and valleys are detected using multi-scale searching windows. The width of the detection segment is also estimated based on the window size. After the initial detections, a contrast filter (greater than 50 HU) and a size filter (greater than 5mm) are applied to eliminate false detections. Figure 6B shows the detection segments on the intensity profile.

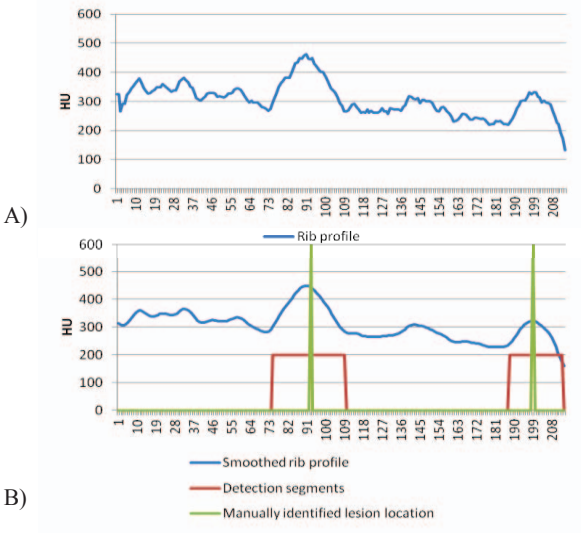


Figure 6. Rib profile and lesion detection. A) Rib profile; B) Smoothed profile and lesion detection.

A set of features are then computed for each detection. Five categories of features are defined.

1. Intensity: mean, standard deviation, contrast to adjacent segments.
2. Position: position along the centerline.
3. Size: length, diameter, volume, area.
4. Shape: circularity, shape moments, curvature.
5. Cortical bone: thickness, density.

The features are then sent to a support vector machine (SVM) [9] for classification. The SVM is trained using visually identified rib lesions. If a detection segment

includes the manually placed lesion mark, it is considered as a true positive, otherwise a false positive.

6. RESULTS

A series of CT scans from 10 patients with studies demonstrating sclerotic metastatic disease in the ribs was gathered. The section thickness of the scans was 5 mm. A total of 185 lesions were identified and marked by an expert radiologist. All patients are male with prostate cancer. The cases were obtained from an electronic medical record search of our radiology information system in the period from Jan 2009 to Dec 2010. The patient ages ranged from 42 to 66 years, with an average of 55 years. Figure 7 depicts the spatial distribution of lesions on a rib centerline rendering in one patient.

A leave-one-out schema is utilized to validate our CAD system for rib lesion detection. We analyze the results of the SVM classifier by plotting a free-response receiver operating characteristic (FROC) curve depicting sensitivities and false positive rates. Figure 8 shows the FROC curve. The sensitivity is 75.4% at 5.6 false positive per case at our selected operating point. Figure 9 shows examples of missed lesions and false positives. Most missed lesions are due to low density and small size, and most false positives are cartilage calcification and volume averaging.

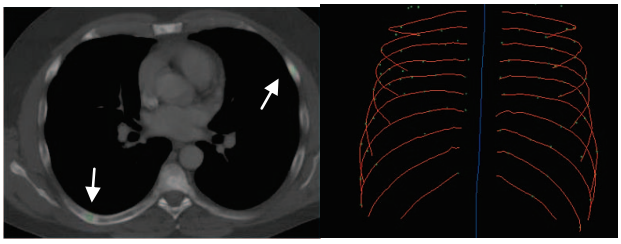
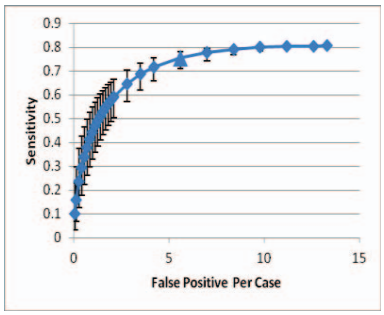


Figure 7. Manually identified lesions on 2D slices and their distribution in 3D. Green dots indicates rib lesions.



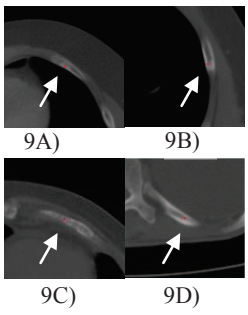


Figure 8. FROC Analysis. The operating point is 75.4% sensitivity at 5.6 false positive per case.

Figure 9. Examples of missed lesions (A, B) and false positives (C, D). A) low density lesion; B) small lesion; C) cartilage calcification; and D) volume averaging.

7. CONCLUSION

We have presented a computer-aided detection system for detecting sclerotic metastatic bone lesions of the ribs on routine CT studies. The technique overcomes the challenges posed by thick slices in routine CT studies. We also developed an intuitive tool to display all ribs and the distribution of lesions in one view. The rib tracing algorithm still needs improvement. Only 10 pairs of ribs can be successfully traced in most cases. The first two pairs of ribs (T1 and T2) have a larger curvature and different cross section shape than the other ribs. Different tracing parameters are required.

This CAD system has potential to increase the sensitivity for initial detection of sclerotic metastatic lesions in the rib, as well as to act as a component system in the assessment of bone tumor burden in cases of known sclerotic bone metastases.

8. ACKNOWLEDGMENTS

This research was supported in part by the Intramural Research Program of NIH, Clinical Center.

9. REFERENCES

[1] G. Mundy, "Metastasis to bone: causes, consequences and therapeutic opportunities," *Nature Reviews Cancer*, vol. 2, pp. 584-593, 2002.

[2] T. Wiese, J. Burns, J. Yao, and R. M. Summers, "Computer-aided detection of sclerotic bone metastases in the spine using watershed algorithm and support vector machines," presented at IEEE International Symposium on Biomedical Imaging, Chicago, IL, 2011.

[3] J. Staal, B. v. Ginneken, and M. A. Viergever, "Automatic rib segmentation and labeling in computed tomography scans using general framework for detection, recognition and segmentation of objects in volumetric data," *Medical Image Analysis*, vol. 11, pp. 35-46, 2007.

[4] T. Klinder, C. Lorenz, J. von Berg, S. Dries, T. Bulow, and J. Ostermann, "Automated Model-Based Rib Cage Segmentation and Labeling in CT Images," presented at MICCAI, 2007.

[5] J. Lee and A. P. Reeves, "Segmentation of Individual Ribs from Low-dose Chest CT," presented at SPIE Medical Imaging, 2010.

[6] A. P. Kiraly, S. Qing, and H. Shen, "A novel visualization method for the ribs within chest volume data," presented at SPIE Medical Imaging, 2006, vol. 6141.

[7] H. Shen, L. Ma, J. Kafer, and D. P. Naicich, "Automatic Detection of Rib Metastasis in Chest CT Volume Data," presented at SPIE Medical Imaging, 2007, vol. 6514.

[8] J. Yao, S. D. O'Connor, and R. M. Summers, "Automated Spinal Column Extraction and Partitioning," presented at IEEE ISBI, Arlington, VA, 2006.

[9] N. Cristianini and J. S. Taylor, *An Introduction to Support Vector Machines*: Cambridge University Press, 2000.